Simulation of Photon-Photon Resonance Enhanced Direct Modulation Bandwidth of DFB Lasers

M. Dumitrescu, T. Uusitalo, H. Virtanen
Optoelectronics Research Centre, Tampere University of Technology
Tampere, Finland,
Mihail.Dumitrescu@tut.fi

A. Laakso
Brighterwave Inc,
Tampere, Finland,
Antti.Laakso@brighterwave.com

P. Bardella, I. Montrosset
Department of Electronics, Politecnico di Torino
Torino, Italy
Paolo.Bardella@polito.it

***Abstract*—Simulations and experimental results of high-frequency photon-photon resonance are used to examine the possibilities to extend the direct modulation bandwidth in dual-mode distributed feedback lasers beyond the conventional limit set by the carrier-photon resonance.**

I. Introduction

Despite the substantial efforts undertaken to increase the laser direct modulation bandwidth, no significant breakthrough has been made when the direct modulation bandwidth has been linked to the carrier-photon resonance (CPR), largely because the CPR has inherent physical limitations. However, since the direct modulation bandwidth can be extended considerably by introducing a supplementary high-frequency resonance of the laser, we have managed to consistently and systematically induce a high-frequency photon-photon resonance (PPR) in order to increase the direct modulation bandwidth of our lasers.

II. Photon-Photon Resonance

A modified rate-equation model has been developed to take the PPR into account by treating the longitudinal confinement factor as a dynamic variable [1]:

$$\frac{d}{dt}\begin{bmatrix} dN \\ dN_p \end{bmatrix} = \begin{bmatrix} -\gamma_{NN} & -\gamma_{NP} \\ \gamma_{PN} & -\gamma_{PP} \end{bmatrix}\begin{bmatrix} dN \\ dN_p \end{bmatrix} + \begin{bmatrix} \frac{\eta_i}{qV} dI \\ (N_p v_g g + R_{sp}^{'}) d\Gamma \end{bmatrix} \quad (1)$$

where γ_{NN}, γ_{NP}, γ_{PN} and γ_{PP} are rate coefficients, as defined in [2]. The modulation transfer function, including the influence of the extra term resulted from the (space and) time variation of the confinement factor, is:

$$H(\omega) = \frac{\eta_i}{qV} \frac{\int_0^T \frac{\gamma_{PN}}{\Delta} dt}{T} + \frac{1}{I_1 \cdot T} \cdot \int_0^T \frac{(\gamma_{NN} + j\omega) \cdot (N_p v_g g + R_{sp}^{'})}{\Delta \cdot e^{j\omega t}} \cdot \frac{d\Gamma}{dt} dt \quad (2)$$

where T is the time interval for which the phase difference between the dominant longitudinal modes is maintained. The first term in (2) resembles the traditional modulation transfer function, with γ_{PN} and Δ taken as time-dependent, while the second term results from considering the (space and) time dependence of the confinement factor. This second term introduces the supplementary PPR peak placed at a frequency equal with the frequency difference between the two dominant longitudinal modes. The model indicates that a primary condition for achieving the PPR is to have the dominant modes phase-locked for long enough (quasi-phase- locked). Therefore, besides the large frequency difference between modes, the main reason for not achieving a significant PPR peak in conventional multimode lasers is that they do not provide a mechanism to maintain the phase difference between modes for long enough.

The difficulty in extending the direct laser modulation bandwidth is not so much related to placing the PPR at high frequencies as it is related to achieving a flat modulation response between the CPR and the PPR.

III. Experimental Results

Multi-section 1.3 and 1.55 μm DFB lasers with 3rd-order laterally-coupled ridge-waveguide (LC-RWG) surface gratings [3] have been fabricated, without regrowth and using cost-effective UV nanoimprint lithography [4], from InP-substrate legacy epiwafers (with epilayer structures designed for Fabry-Perot lasers). Structural variations of the lasers enabled the emission of two quasi-phase-locked longitudinal modes with frequency differences ranging from 14 GHz to 1.3 THz. Fig. 1a and 1b show measured and simulated dual-mode emission spectra with a frequency separation of 47 GHz and 1 THz, respectively.

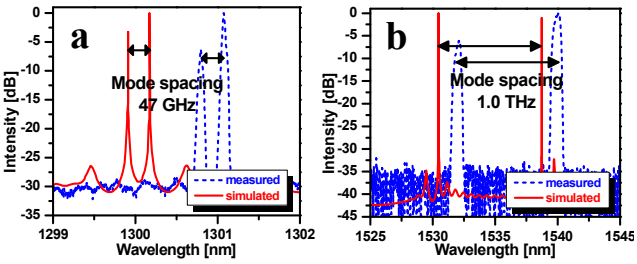

Fig. 1. Simulated and measured dual-mode emission spectra with quasi-phase-locked longitudinal modes having (a) 47 GHz and (b) 1.0 THz frequency spacing

Because the modulation responses of the dual-mode lasers with big frequency differences between the two quasi-phase-locked modes are hampered by the large and deep dip between the CPR and the PPR, we have targeted mainly PPR frequencies below and around 20 GHz. Two types of DFB lasers have been fabricated in the same fabrication run and from the same legacy epiwafer (with the epilayer structure intended for the fabrication of Fabry-Perot lasers at 1.55 μm).

978-1-4673-8603-6/16/$31.00 ©2016 IEEE

The first type was a single-mode DFB laser with LC-RWG gratings, which does not exhibit PPR. The second type was a much longer multiple-longitudinal-section DFB laser with similar LC-RWG gratings, having a longitudinal structure designed to induce PPR at ≈ 14 GHz. Fig. 2 shows measured and simulated direct modulation responses for both types of lasers, illustrating the increase in small-signal modulation bandwidth obtained by exploiting the photon-photon resonance. The modulation response simulation for the laser with PPR was fitted to the measurement by assuming a SMSR of 23 dB between the two quasi-phase-locked modes.

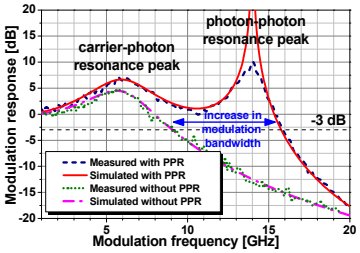

Fig. 2. Measured and simulated small-signal modulation responses for two types of lasers, one without PPR and the other with PPR at 14 GHz.

We have studied the possibility to adjust the PPR position and the flatness of the modulation response between the CPR and PPR by adjusting the bias currents of the laser sections. Fig. 3a and 3b show the tuning of the PPR frequency (and the CPR changes) induced by adjusting one of the bias currents for a 1.6 mm long multi-section DFB laser emitting at 1.55 µm and for a 1.5 mm long multi-section DFB laser emitting at 1.3 µm, respectively. It can be observed how the CPR-PPR gap is filled when the PPR is brought closer to the CPR.

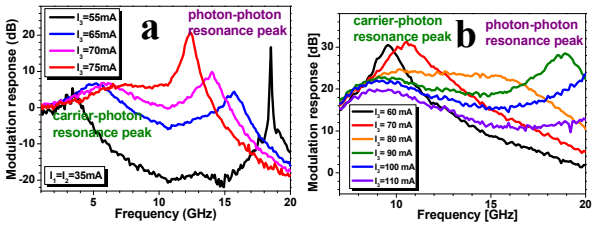

Fig. 3. Measured small-signal modulation response with the PPR position adjusted by the bias applied to one of the laser sections in: (a) 1.6 mm long multi-section laser with LC-RWG gratings emitting at 1.55 µm, (b) 1.5 mm long multi-section laser with LC-RWG gratings emitting at 1.3 µm.

Since the -3 dB small-signal modulation bandwidth may not be indicative of the large-signal modulation capability, particularly in case of a small-signal modulation response with substantial variations across the bandwidth, we have also analyzed the small-signal modulation response and the corresponding large-signal modulation capability using a Finite-Difference Travelling-Wave program [5]. Fig. 4ss shows the small-signal modulation response simulated for three different phases of the cleaved-facet mirror reflectivity in a multi-section laser (a similar result can be obtained by changing the bias current in one of the laser sections).

Large-signal eye diagrams were calculated for the three values of cleaved-facet reflectivity phase, using a non-return-to-zero pseudorandom bit sequence signal at different modulation bit rates. The cases were chosen to compare the situation when the PPR peak is small, under the -3 dB level and with minimal influence on the -3 dB small-signal modulation bandwidth (case A); the situation when the PPR peak is moderate and the modulation response is extended in a relatively flat way (case B); and the situation when the PPR peak is very pronounced (case C).

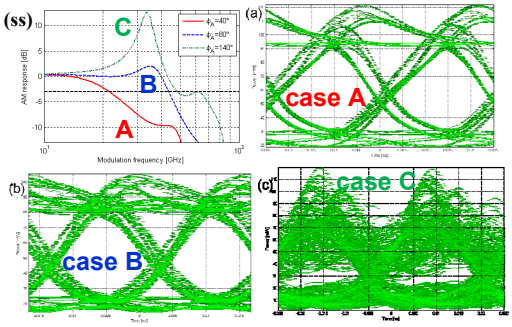

Fig. 4. (ss) Simulated small-signal modulation response for different phases of the cleaved facet mirror reflectivity in a multi-section laser with high-frequency PPR; (a) 40Gb/s eye diagram computed for case A, having an extinction ratio (ER) = 6dB; (b) 60Gb/s eye diagram computed for case B, having ER = 4.5dB; (c) 40Gb/s eye diagram computed for case C.

In case B, as expected, an eye diagram with a reasonably good extinction ratio (ER = 4.5 dB) could be obtained beyond the -3 dB small-signal modulation bandwidth, at 60 Gb/s. The simulations also confirm that a strong PPR peak (case C) is dramatically reducing the eye opening at 40 Gb/s, although a good large-signal modulation response should be achieved at this rate if the small-signal modulation response would be flat. Surprisingly, a good 40 Gb/s large-signal modulation response, beyond the –3 dB small-signal modulation bandwidth, could be obtained in the case A, when the PPR peak is well below the -3 dB level and does not influence substantialy the small-signal modulation bandwidth. This result indicates a significantly broader operational range where the large-signal modulation capability can be extended by exploiting the PPR.

IV. Conclusions

Our simulation and experimental results prove that the PPR can be exploited for increasing the laser direct modulation bandwidth beyond the limitations set by the carrier-photon resonance.

References

[1] A. Laakso, M. Dumitrescu, "Modified rate equation model including the photon-photon resonance", *Opt. Quantum Electron*, Vol. 42, No. 11-13, pp. 785-791I, 2011.

[2] L.A. Coldren and S.W. Corzine, "Diode Lasers and Photonic Integrated Circuits", Wiley, New York, 1995.

[3] A. Laakso, M. Dumitrescu, et al., "Optical modeling of laterally-corrugated ridge-waveguide gratings ", *Opt. Quantum Electron*, vol. 40, No. 11-12, pp. 907-920, 2008.

[4] J. Viheriälä, M-R. Viljanen, J. Kontio, T. Leinonen, J. Tommila, M. Dumitrescu, T. Niemi and M. Pessa, "Soft stamp ultraviolet-nanoimprint lithography for fabrication of laser diodes", *J. Micro/Nanolith.*, Vol. 8, No. 3, pp. 033004/1-8, 2009.

[5] P. Bardella, I. Montrosset, "Design and simulation of DBR lasers with extended modulation bandwidth exploiting photon-photon resonance effect", Proc. ECIO'2012, pp. 212-214, 2012.